



SEPTEMBER 15 2023

## An overview of acoustical measurements made of the Atlas V JPSS-2 rocket launch

Logan T. Mathews ; Mark C. Anderson; Carson D. Gardner; Bradley W. McLaughlin; Brooke M. Hinds; Megan R. McCullah-Boozer; Lucas K. Hall; Kent L. Gee 



*Proc. Mtgs. Acoust.* 51, 040003 (2023)

<https://doi.org/10.1121/2.0001768>



View  
Online



Export  
Citation

CrossMark



 **ASA**

Advance your science and career as a member of the  
**Acoustical Society of America**

[LEARN MORE](#)



## 184th Meeting of the Acoustical Society of America

Chicago, Illinois

8-12 May 2023

### \*Noise: Paper 1aNS9

## An overview of acoustical measurements made of the Atlas V JPSS-2 rocket launch

**Logan T. Mathews, Mark C. Anderson, Carson D. Gardner and Bradley W. McLaughlin**

*Department of Physics and Astronomy, Brigham Young University, Provo, UT, 84602;  
loganmathews103@gmail.com; anderson.mark.az@gmail.com; cgard25@byu.edu; mclau4@byu.edu*

**Brooke M. Hinds, Megan R. McCullah-Boozer and Lucas K. Hall**

*Department of Biology, California State University Bakersfield, Bakersfield, CA, 93311; bhinds@csu.edu;  
mmccullah@csu.edu; lhall12@csu.edu*

**Kent L. Gee**

*Department of Physics and Astronomy, Brigham Young University, Provo, UT, 84602; kentgee@byu.edu*

On 10 November 2022, measurements were made of the Atlas V JPSS-2 rocket launch from SLC-3E at Vandenberg Space Force Base, California. Measurements were made at 11 stations from distances of 200 m to 7 km from the launch pad. Measurement locations were arranged at various azimuthal angles relative to the rocket to investigate possible noise asymmetry. This paper discusses preliminary results from this measurement including overall levels, temporal and spectral characteristics, evidence of nonlinear propagation, and potential azimuthal asymmetry effects.

*\*POMA Student Paper Competition Winner*



## 1. INTRODUCTION

In an era when the space launch industry is experiencing rapid growth, proper understanding of rocket launch acoustics is of ever-growing importance<sup>1</sup>. With increased launch cadence and the construction of new launch facilities, the understanding and modeling of rocket noise is vital to the design of rockets and payloads, pad and ground facilities design, and environmental and community noise assessments. To this end, acoustical measurements of rocket launches can inform noise models and regulations<sup>2</sup>. This paper gives an overview of one such measurement of a medium-lift orbital rocket launch and explores some of the basic acoustic characteristics observed.

Since most launch vehicles in use today have multi-nozzle configurations, understanding the associated effects on the acoustic radiation is important. This becomes particularly relevant when there is asymmetry in the nozzle configuration which creates the possibility for plume shielding, resulting in the potential for azimuthal asymmetry in the noise radiation. While the jet noise community has studied clustered jet effects widely, studies particular to rocket noise have been sparse. Several numerical and experimental studies on supersonic jets have shown an effective shielding of overall levels on the order of 2-3 dB in twin jets<sup>3-6</sup>.

Eldred et al.<sup>7</sup> proposed a model for the flow characteristics of multi-nozzle jet noise flows. For jets spaced closer than 3 nozzle diameters, a two-zone model for noise production was proposed. The radiated noise was expected to consist of single-nozzle type radiation originating from the portion of the flow upstream of where coalescence begins and combined-nozzle type radiation originating farther downstream where the flows have effectively coalesced. This results in a double-peaked spectrum, with the higher frequency peak corresponding to single-nozzle behavior and a lower frequency peak corresponding to the combined flow. Kandula<sup>8</sup> successfully applied this model in conjunction with the propagation methodology from Eldred<sup>9</sup> (NASA SP-8072) to predict sound pressure level spectra from a clustered-nozzle rocket configuration. Potter and Crocker<sup>10</sup> extended Eldred's methodology to rocket noise but noted its inherent limited characteristics; namely that the computation assumes a flow of constant density and that rocket exhausts are much more extreme in temperature, velocity, etc. than turbojets.

The purpose of this paper is to document the acoustical measurement of the Atlas V JPSS-2 launch and to publish relevant preliminary findings. An analysis of the ignition overpressure event is shown, with azimuthal variability in peak levels being shown to correspond with the flame trench orientation. Maximum overall levels are shown, and a simple method for predicting this parameter is shown to be accurate at all stations with an uncertainty of  $\pm 2.5$  dB. Evidence of nonlinearity in signals is shown. Spectral characteristics are discussed. Evidence for and against azimuthal asymmetry in launch noise due to the nozzle configuration is discussed, both in terms of maximum overall levels and spectral peak frequency.

## 2. METHODS

### A. LAUNCH VEHICLE

The Atlas V is a medium- to heavy-lift launch vehicle developed and operated by United Launch Alliance. A diagram of the Atlas V rocket is shown in Fig. 1. It is the last member of the Atlas rocket family, which originated with the SM-65 Atlas ballistic missile in 1957. As of this article's publication, 97 Atlas V rockets have launched from two launch facilities: SLC-3E at Vandenberg Space Force Base (VSFB) and SLC-41 at Cape Canaveral Space Force Station (CCSFS). For this launch, the Atlas V vehicle was in the 401 configuration (four-meter fairing, no solid rocket boosters, and one RL10C-1 engine on the Centaur upper stage). Thus, the entirety of the first-stage thrust was generated by the RD-180 engine. The RD-180 engine, developed from the RD-170, is produced by NPO Energomash and is a single-engine unit with two closely spaced nozzles of diameter  $D = 1.43$  m, each with a combined maximum thrust of 3.83 MN at sea level<sup>11</sup>. The equivalent diameter of a single nozzle with the same exit area as the two nozzles of the RD-180 is defined as  $D_e = D\sqrt{2} = 2.02$  m. The approximate center-to-center distance between the nozzles is estimated to be approximately 1.63 m, which results in  $S/D \approx 1.14$ .

## Atlas V 401 Rocket

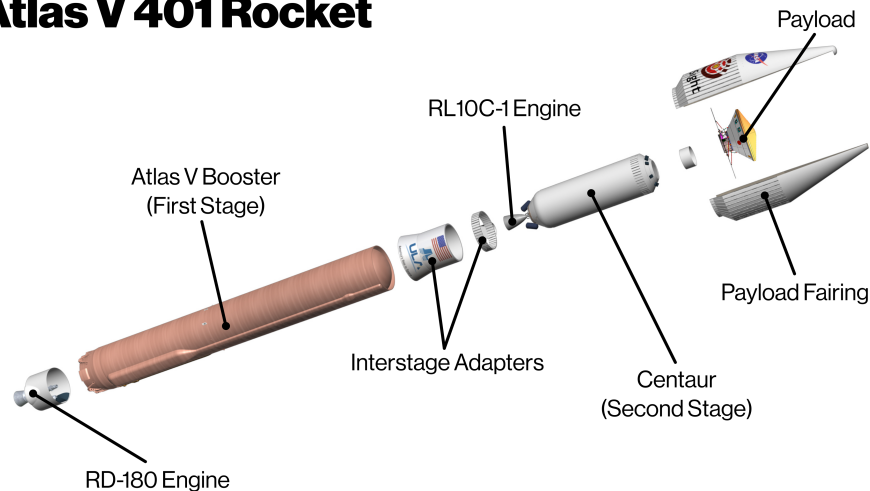


**Figure 1.** Atlas V 401 rocket diagram. Base image credit: NASA/JPL-Caltech. Public domain.

For reference, an azimuthal coordinate system relative to the rocket nozzle configuration has been defined for this analysis. A graphical overview of the coordinate system is presented in Fig. 2. The azimuthal angle  $\varphi$  indicates the orientation of the observer relative to the nozzles. At  $\varphi = 0^\circ$ , the observer sees the two nozzles broadside (Fig. 2b), whereas at  $\varphi = 90^\circ$ , the observer sees only one nozzle (Fig. 2c).

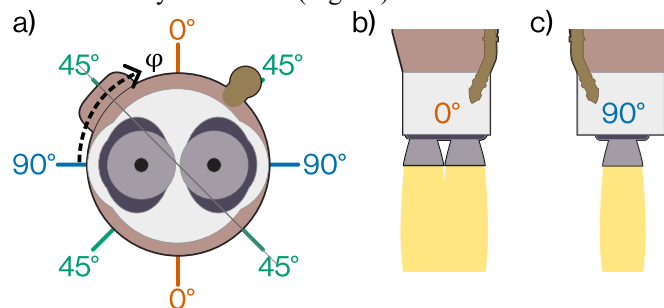


**Figure 2.** a) Orientation of rocket nozzles with the angle  $\varphi$  in the defined coordinate system. b) At  $\varphi = 0^\circ$ , the observer sees two nozzles and cores broadside. c) At  $\varphi = 90^\circ$ , the observer sees one nozzle/core end-on.

### B. MEASUREMENT

On 10 November 2022 at 01:49 AM PST (09:49 AM UTC), an Atlas V 401 rocket lifted off from SLC-3E at Vandenberg Space Force Base, California, USA carrying the Joint Polar Satellite System (JPSS)-2 and Low-Earth Orbit Flight Test of an Inflatable Decelerator (LOFTID) payloads. Measurements were conducted at 11 primary stations, strategically placed around the rocket at radial distances ranging from 217 m to 7.2 km radially from the launch pad. Figure 3 shows the layout of these measurement locations, with the rocket axes defined in Fig. 2 shown. This measurement configuration is similar to a measurement conducted of the Atlas V Landsat 9 launch from the same facility, discussed by Cunningham et al.<sup>12</sup>. However, it should be noted that in the measurement by Cunningham et al., the measurement axes were defined relative to the Mobile Service Tower. However, the vehicle was discovered to be rotated by  $\sim 22^\circ$  with respect to the building. This misalignment was noticed after the launch, and the axes were corrected in this measurement to align with the rocket properly.

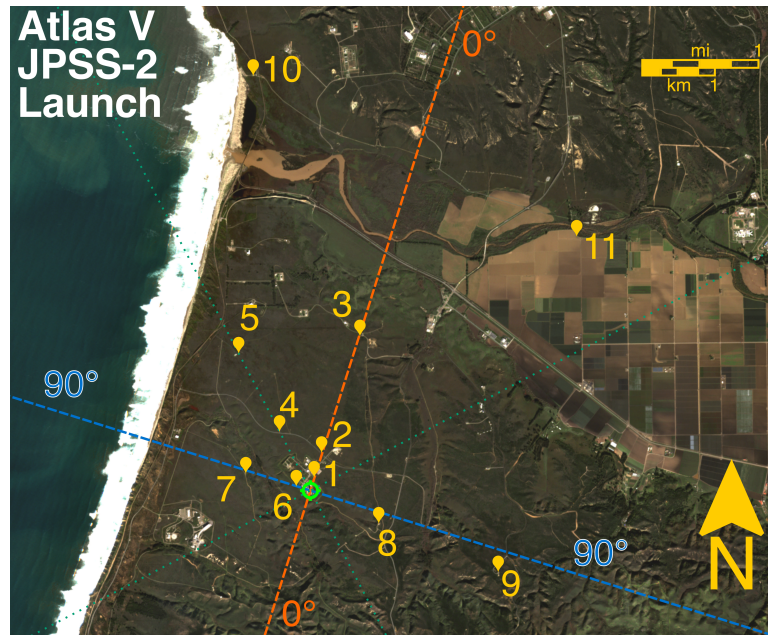


**Figure 3. Map of measurement station locations at JPSS-2 launch. Station numbers and rocket axes are indicated.**

A summary of each of the 11 measurement stations is reported in Table 1. The horizontal distance from the launch facility to the measurement location is reported as  $d$ . The actual angle with respect to the rocket axes,  $\varphi$ , is reported, as well as the approximate angle  $\tilde{\varphi}$  (within  $\sim\pm 10^\circ$ ) for convenience in discussing similar angular site groupings.

**Table 1. Station information with distances relative to the launch pad and angles in the described coordinate system.**

Station	$d$ (m)	$\varphi$	$\tilde{\varphi}$
1	217	$2^\circ$	$0^\circ$
2	656	$4^\circ$	$0^\circ$
3	2800	$2^\circ$	$0^\circ$
4	1080	$47^\circ$	$45^\circ$
5	2650	$47^\circ$	$45^\circ$
6	283	$89^\circ$	$90^\circ$
7	1118	$87^\circ$	$90^\circ$
8	1368	$79^\circ$	$90^\circ$
9	3625	$82^\circ$	$90^\circ$
10	7250	$24^\circ$	$30^\circ$
11	6430	$31^\circ$	$30^\circ$

Measurements were made with a mixture of custom PUMA (Portable Unit for Measuring Acoustics) systems, which consist of NI CompactDAQ data acquisition modules, a portable computer system running custom data acquisition software, and batteries for power<sup>13</sup>. Due to limited hardware resources at the time of the measurement, GPS time clocks were unavailable for absolute time synchronization across stations at this measurement. In addition to PUMA systems, Larson Davis 831C sound level meters were used at some locations, which recorded acoustic data as an uncompressed *WAV* file at a sample rate of 51.2 kHz and which has been determined to be of sufficient fidelity for rocket noise applications<sup>14</sup>. All systems had microphones placed in a custom ground plate/windscreen setup, referred to at BYU as a COUGAR (compact outdoor unit for ground-based acoustical recordings, see Anderson et al.<sup>15</sup>). Figure 4 shows the instrumentation setups at two representative stations. The COUGAR microphone setup can be seen in each, along with the instrumentation box and portable weather monitoring equipment on tripods.



**Figure 4.** (Left) Station 7 at 1.1 km. (Right) Station 6 at 283 m. In both images, the launch facility Mobile Service Tower is visible, and within it is the rocket. Also visible in the foregrounds are the microphone ground plate/windscreen setups, instrumentation boxes, and weather stations.

### 3. RESULTS

#### A. IGNITION OVERPRESSURE (IOP)

Ignition of the RD-180 engines on the Atlas V vehicle produces an ignition overpressure (IOP) event with a characteristic signature. Waveforms containing the IOP are shown for stations 1-9 in Fig. 5. The IOP signature for the Atlas V is unique; it produces a noticeable whooshing sound unlike IOPs observed on other vehicles such as the Falcon 9 and Space Launch System, which produce a more impulse-like signature. The unique behavior of this IOP is also shared with the Antares vehicle launched from the Mid-Atlantic Regional Spaceport. It is possible that the configuration of the flame trench could allow for strong resonances to be excited by the IOP event, producing the characteristic sound. It is also worth noting that the Antares vehicle uses RD-181 engines, which are largely the same as the RD-180 used on the Atlas V. Thus, the unique IOP signature of the Atlas V and Antares vehicles could also be related to the engines themselves.

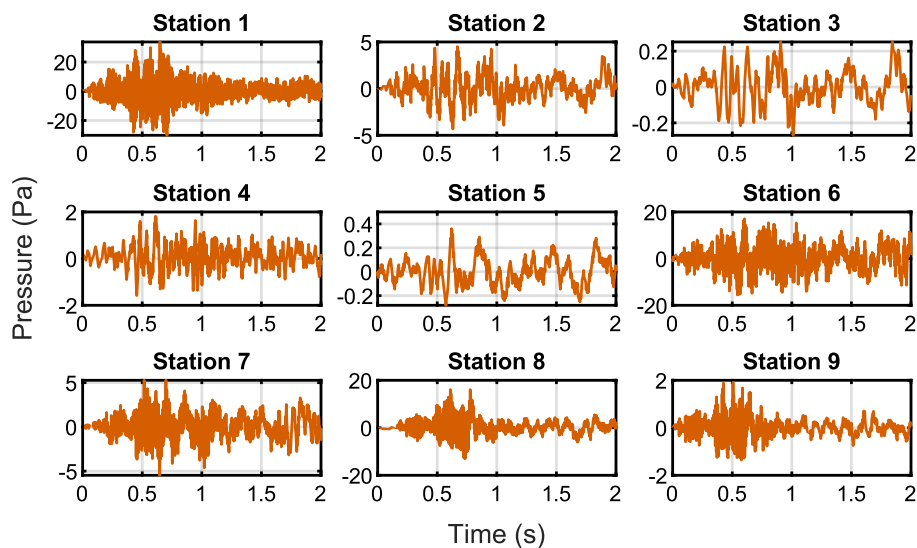


**Figure 5.** Ignition overpressure (IOP) waveform signatures from stations 1-9.

Figure 6 shows the peak sound pressure level ( $L_{pk}$ ) associated with the IOP event at stations 1-9, relative to the mean  $L_{pk}$  across these stations. All levels have been scaled for spherical spreading to  $100D_e$ . The direction of the flame trench exit is indicated by the red dashed line. There is considerable azimuthal asymmetry in the scaled peak IOP levels. Stations closest to the flame trench exit azimuth consistently have a higher  $L_{pk}$  than average, with station 8 being 16 dB greater than the mean  $L_{pk}$ . Opposite the flame trench exit, there are consistently lower-than-average peak levels, with the lowest being 14 dB lower than average. This indicates a scaled variability of 30 dB in the IOP  $L_{pk}$ , which is considerable. Similar IOP asymmetry corresponding to the flame trench direction was noticed by Gee et al.<sup>16</sup> with the Space Launch System vehicle. This observation reinforces the understanding that significant IOP directionality exists with flame trenches, which should be considered when designing launch facilities and evaluating the environmental and ecological effects of rocket launches.

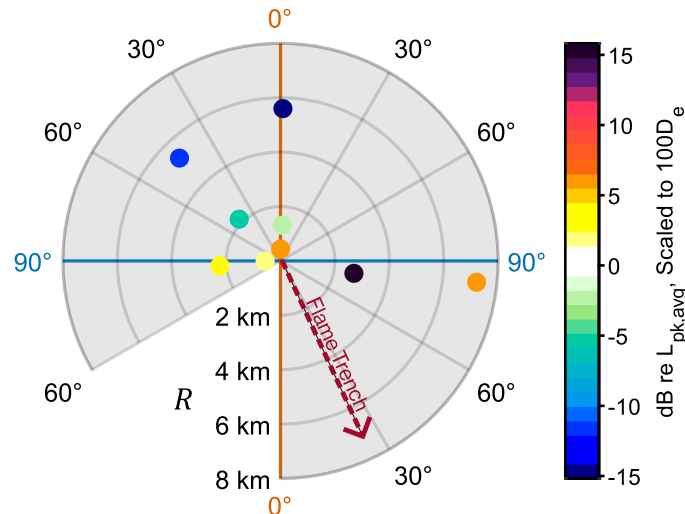


**Figure 6.** Ignition overpressure (IOP) peak levels, relative to the average across all depicted sites, adjusted for geometric spreading to  $100D_e$  (202 m) from the launch pad. The direction of the flame trench exit is indicated by the dashed red line.

## B. OVERALL SOUND PRESSURE LEVELS

Figure 7 shows the maximum 1-s averaged overall sound pressure levels ( $OASPL_{max}$ ) as a function of distance to the source (the distance being calculated assuming a peak overall directivity angle of  $65^\circ$ ). Note that all levels reported in this discussion are referenced to  $20 \mu\text{Pa}$  unless otherwise noted. Also shown are the  $OASPL_{max}$  values adjusted for ground effects (triangular blue markers) by provisionally subtracting 6 dB from the level. This is a reasonable correction for the overall level as discussed by Hart et al.<sup>17</sup>, since the majority of rocket noise energy is concentrated at sufficiently low frequencies that typical ground surfaces essentially create a pressure-doubling effect at the microphone.

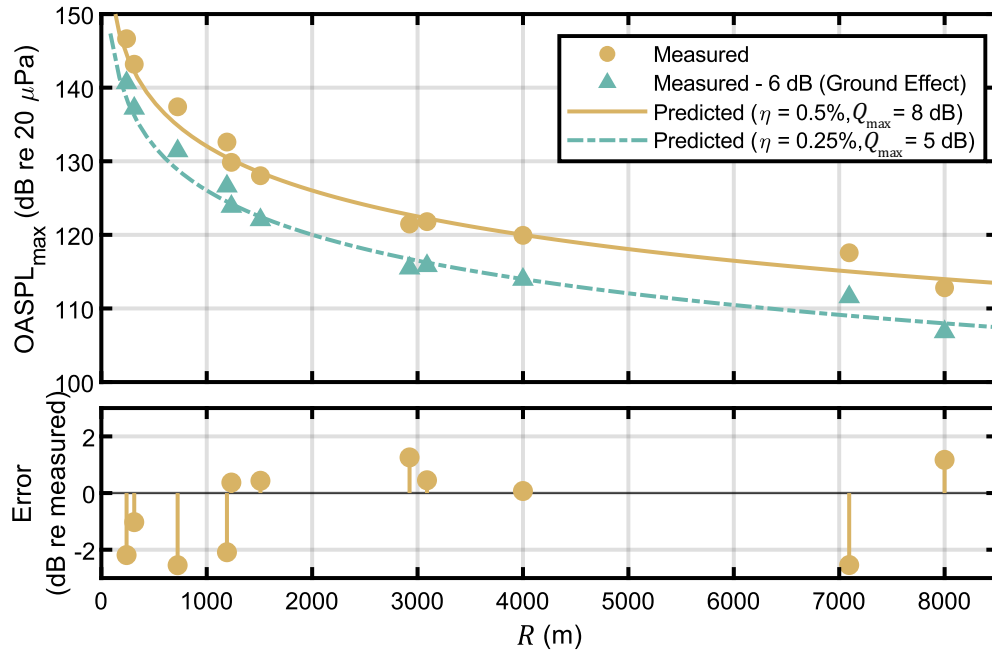


**Figure 7. (Top) Maximum overall sound pressure levels as measured, compared with the prediction method of Eq. (1). Also shown are levels adjusted for ground effects and an adjusted prediction. (Bottom) Difference between measurement and prediction at each station.**

Also shown in Fig. 7 are curves representative of a simple predictive method for  $OASPL_{max}$  of a rocket. The maximum overall sound pressure level of a launch vehicle at a given distance from the rocket may be approximated by the expression

$$\begin{aligned} OASPL_{max} &= 10 \log_{10} \left( \frac{\eta W_m}{10^{-12} W} \right) - 20 \log_{10}(4\pi R^2) + Q_{max} \\ &= OAPWL - 20 \log_{10}(4\pi R^2) + Q_{max}, \end{aligned} \quad (1)$$

where  $\eta$  is an acoustic efficiency ( $\eta = W_a/W_m$ ) and  $W_m$  is the mechanical power, taken to be approximately equal to  $\frac{1}{2}TU_e$ , where  $T$  is the total thrust and  $U_e$  is the engine exit velocity. In Eq. (1),  $R$  is the distance to the source which is the distance to the launch site. Assuming an overall angle of maximum radiation of  $65^\circ$ , the relationship between these variables can be expressed as  $R = d/\sin 65^\circ$ .

This model, first applied to rocket noise by McInerney<sup>18</sup>, combines three elements: the estimation of acoustic power from the mechanical power of the rocket by assuming an acoustic efficiency, accounting for spherical spreading (which gives the maximum overall sound pressure level for an equivalent monopole), and finally accounting for directionality by adding on a maximum directivity index  $Q_{max}$ . Historically, an efficiency of  $\eta = 0.5\%$  has been assumed with a maximum directivity index of  $Q_{max} = 8$  dB. However, accounting for ground reflections and applying a provisional decrease in measured pressures by a factor of two, the estimate for acoustic efficiency would then be reduced by a factor of two as well, which yields  $\eta \approx 0.25\%$ . This adjustment also affects the calculation of  $Q_{max}$ , which would become  $Q_{max} = 5$  dB. Using these adjusted values, the predicted maximum overall sound pressure levels now match closely the measured data that has been adjusted for ground effects.

This model was also used earlier by Franken<sup>19</sup> for turbojet noise, however, the geometric spreading term differed by treating the radiation as a half-space problem ( $2\pi R^2$ , hemispherical spreading) instead of a free-space problem ( $4\pi R^2$ , spherical spreading) due to the presence of the ground. It is worth noting that the formulation in Eq. (1) makes no provision to correct for ground effects, but also treats the problem as free space (hence the  $4\pi R^2$ ). If Eq. (1) is adjusted to half-space, this changes the value of  $Q_{max}$  to be 5 dB instead of 8 dB. Since the acoustic efficiency is a property of the source regardless of whether the half- or free-space problem is considered, we can conclude that  $\eta \approx 0.25\%$ . Hence, the maximum overall level without accounting for ground effects (half-space) becomes



$$\begin{aligned} OASPL_{max, half} &= 10 \log_{10} \left( \frac{\eta W_m}{10^{-12} W} \right) - 20 \log_{10}(2\pi R^2) + Q_{max} \\ &= OAPWL - 20 \log_{10}(2\pi R^2) + Q_{max}, \end{aligned} \quad (2)$$

and the maximum overall level accounting for ground effects (free space) is

$$\begin{aligned} OASPL_{max, free} &= 10 \log_{10} \left( \frac{\eta W_m}{10^{-12} W} \right) - 20 \log_{10}(4\pi R^2) + Q_{max} \\ &= OAPWL - 20 \log_{10}(4\pi R^2) + Q_{max}. \end{aligned} \quad (3)$$

In both cases, then,  $\eta \approx 0.25\%$  and  $Q_{max} = 5$  dB, which reflects these quantities being fundamental source properties unaffected by the presence or absence of the ground.

The predicted values for  $OASPL_{max}$  underestimate the true level slightly on average. However, there is not a consistent bias visible in the error between the measurement and the prediction in Fig. 7. Generally, the model predicts  $OASPL_{max}$  accurately within a  $\pm 2.5$  dB margin of error<sup>i</sup>. For a simplistic model that has no inclusion of propagation, nonlinear, or terrain effects, this performance is satisfactory. McNerny previously applied the same model across 5 rocket launches (4 distinct vehicles) with a considerably larger relative error of  $\pm 6.4$  dB<sup>ii</sup>.

To investigate potential azimuthal asymmetry effects on the overall maximum level, Table 2 shows the measured  $OASPL_{max}$  at each station, as well as the  $OASPL_{max}$  scaled for geometric spreading to a common distance of  $100D_e = 202$  m from the source. Also shown is the scaled  $OASPL_{max}$  values relative to the average. There appears to be no apparent discernable bias in levels between  $\tilde{\varphi} = 0^\circ$  and  $90^\circ$  that is greater than the variation observed in each angular grouping.

**Table 2.  $OASPL_{max}$  and  $OASPL_{max}$  scaled for geometric spreading to a common distance of  $100D_e$ .**

Station	$d$ (m)	$R$ (m)	$\tilde{\varphi}$	$OASPL_{max}$	$OASPL_{max}$ (Scaled to $100D_e$ )	dB re average $OASPL_{max}$
1	217	239	$0^\circ$	146.7	148.1	1.5
2	656	724	$0^\circ$	137.4	148.5	1.9
3	2800	3090	$0^\circ$	121.8	145.5	-1.1
4	1080	1192	$45^\circ$	132.6	148.0	1.4
5	2650	2924	$45^\circ$	121.5	144.7	-1.9
6	283	312	$90^\circ$	143.2	147.0	0.4
7	1118	1234	$90^\circ$	129.9	145.6	-1.0
8	1368	1509	$90^\circ$	128.0	145.5	-1.1
9	3625	4000	$90^\circ$	119.9	145.9	-0.7
10	7250	8000	$30^\circ$	112.8	144.8	-1.8
11	6430	7095	$30^\circ$	117.6	148.5	1.9

### C. SPECTRAL CHARACTERISTICS

Representative third-octave band maximum launch noise spectra are shown in Fig. 8. The maximum spectra are generated from the region where the noise is within 3 dB of the maximum overall level. Results are shown for the mid-field (Fig. 8a) and far-field (Fig. 8b) at  $\tilde{\varphi} = 0^\circ$  and  $90^\circ$ . The levels of each spectrum have been adjusted for spherical spreading to a common radial distance of  $100D_e = 202$  m. Visible in each spectrum is a high-frequency slope corresponding roughly to  $f^{-2}$  (-10 dB/decade in a one-third octave sense), which is understood to correspond to acoustic shocks in the time domain<sup>20</sup>. Noticeably, this slope rolls off in the far-field at around 2-3 kHz, whereas in

<sup>i</sup> Error max/min: +1.3/-2.5 dB, average (signed/absolute): -0.6/1.3 dB, rms: 1.6 dB; number of data points: 11.

<sup>ii</sup> Error max/min: +6.4/-4.7 dB, average (signed/absolute): 2.0/3.6 dB, rms: 4.0 dB; number of data points: 19.

the mid-field, the shock-correlated slope continues through 20 kHz. This is evidence of the evolution and decay of shocks from the mid- to far-field, where the shock strength has decayed as atmospheric absorption begins to dominate at the higher frequencies<sup>21</sup>.

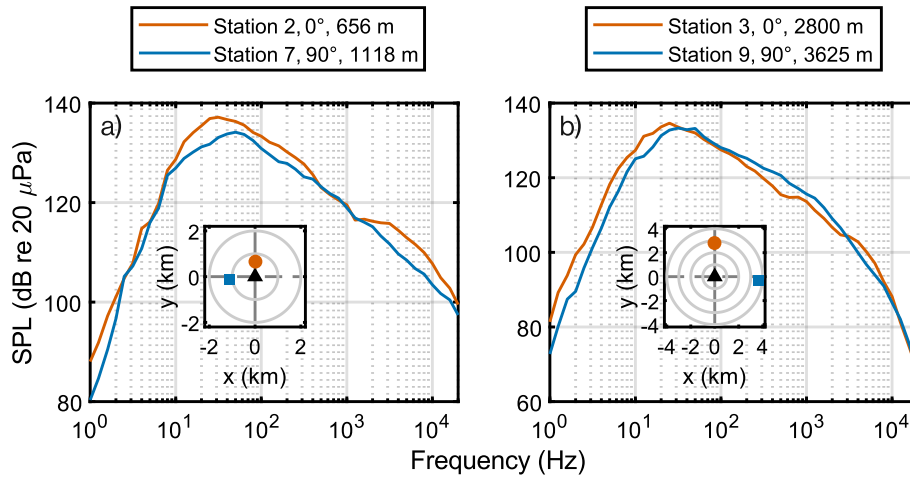


Figure 8. Spectra from 0° and 90° for a) mid- and b) far-field locations.

A noticeable feature in these spectra is the shifting in spectral peak frequency with azimuthal angle  $\tilde{\varphi}$ . The peak frequency at  $\tilde{\varphi} = 90^\circ$  occurs at a higher frequency than  $\tilde{\varphi} = 0^\circ$ . This is summarized in Table 3, where the peak frequencies for all stations at  $\tilde{\varphi} = 0^\circ$  and  $\tilde{\varphi} = 90^\circ$  are shown.

Table 3. One-third-octave peak frequency for each station at  $\tilde{\varphi} = 0^\circ, 90^\circ$ .

Station	$\tilde{\varphi}$	$f_{pk}$
1	0°	40
2	0°	31.5
3	0°	25
6	90°	50
7	90°	50
8	90°	40
9	90°	31.5

If these observed changes in peak frequency are related to single plume/merged plume behavior at  $\tilde{\varphi} = 90^\circ$  and  $0^\circ$ , respectively, it would be expected that a Strouhal number scaling of the peak frequency could account for this effect since a characteristic diameter is included in the nondimensionalization. The classical Strouhal number used in jet noise is given by the expression

$$Sr = \frac{fD_c}{U_c}, \tag{4}$$

where  $f$  is the frequency,  $D_c$  is a characteristic diameter (typically taken to be  $D$  or  $D_j$  for jets), and  $U_c$  is a characteristic flow velocity (typically taken to be  $U_e$  or  $U_j$  for jets). If true merged-plume behavior is present at  $\tilde{\varphi} = 0^\circ$  (observing both plumes broadside), then the characteristic diameter should be  $D_c = D_e = D\sqrt{2}$ . Likewise, for an observer at  $\tilde{\varphi} = 90^\circ$ , only one plume is visible with the other being shielded from view, so the characteristic diameter is expected to be that of just one nozzle  $D_c = D$ . Using these different characteristic diameters in calculating the mean and median peak Strouhal number for  $\tilde{\varphi} = 0^\circ$  and  $90^\circ$ , the results in Table 4 show that for both the mean and median frequencies, the calculated Strouhal numbers for  $\tilde{\varphi} = 0^\circ$  and  $90^\circ$  are nearly identical. This suggests that the shift in peak frequency does appear to be related to a change in characteristic diameter corresponding to single and merged-plume behavior. While this link is promising, more data are needed to strengthen this hypothesis.

**Table 4. Mean and median one-third octave peak frequency at all sites for  $\tilde{\varphi} = 0^\circ, 90^\circ$ . Mean and median Strouhal numbers, computed using the indicated characteristic diameters are also shown.**

$\tilde{\varphi}$	Mean( $f_{pk}$ )	Median( $f_{pk}$ )	$D_c$	Mean( $Sr_{pk}$ )	Median( $Sr_{pk}$ )
$0^\circ$	32.2	31.5	$D_e = D\sqrt{2}$	0.0195	0.0191
$90^\circ$	42.9	45	$D$	0.0184	0.0193

While the peak frequency noticeably shifts, the portions of the spectra above and below the peak frequency do not appear to shift to the same degree. Instead, at  $\tilde{\varphi} = 0^\circ$  a lower frequency “bump” is added to the spectrum, corresponding to the merged plume, which alters the peak frequency of the spectrum while keeping the remaining portions of the spectrum largely the same. This is especially visible in Fig. 8a. Coltrin et al.<sup>22</sup> noticed a similar phenomenon in a laboratory experiment, where as merged plume behavior began to dominate, a lower-frequency peak corresponding to the equivalent diameter appeared and began to dominate the single-nozzle frequency peak. This addition of a lower-frequency spectral peak also mirrors the two-zone model for clustered jets by Eldred et al.<sup>7</sup> and Kandula<sup>8</sup>, which predicts a double-peaked spectrum for clustered jet flows. It is worth noting that this model incorporates no provisions for azimuthal variation. While the spectra shown in Fig. 8 do not appear to exhibit explicit double-peaked behavior, this could be due to the peaks not being well separated. Since the nozzles are relatively closely spaced on the Atlas V ( $S/D \approx 1.14$ ), the radiation coming from the unmerged portion of the plume may be relatively weak as the plumes merge rather quickly; thus at  $\tilde{\varphi} = 0^\circ$ , merged plume behavior with a lower characteristic frequency may dominate the higher frequency peak corresponding to unmerged (single) plume behavior. Further measurements are required to verify this theory.

## 4. CONCLUSION

An acoustical measurement of the Atlas V JPSS-2 launch has been conducted. Measurements were made at 11 stations, ranging in distance from 217 to 7250 m from the launch site at a variety of azimuthal angles. Significant asymmetry of the ignition overpressure peak sound pressure level was observed. This asymmetry corresponded to the flame trench orientation; the distance-scaled peak sound pressure level was observed to be up to  $\sim 30$  dB higher at locations near the flame trench exit azimuth than those opposite this direction.

A simple directional source model predicted the maximum overall sound pressure level at all 11 sites accurately within  $\pm 2.5$  dB. This model, accounting for ground effects, assumed an acoustic efficiency of  $\eta \approx 0.25\%$  and a maximum directivity index of  $Q_{max} = 5$  dB.

During the launch, the maximum overall sound pressure level appeared to not correlate with the orientation of the nozzles with respect to the observer. However, where two nozzles were visible to the observer, the spectral peak frequency was lower. By applying Strouhal number scaling, the spectral peak frequencies were shown to correspond to single-plume behavior where only one nozzle was visible and combined-plume behavior where two nozzles were visible. This suggests that asymmetric clustered nozzle configurations may have different spectral characteristics depending on the orientation of the observer with respect to the nozzles. Further research into different nozzle configurations is warranted to quantify any possible effects.

## ACKNOWLEDGMENTS

This research was supported in part by appointments of L. T. M. and M. C. A. to the Department of Defense (DOD) Research Participation Program administered by the Oak Ridge Institute for Science and Education (ORISE) through an interagency agreement between the U.S. Department of Energy (DOE) and the DOD. ORISE is managed by ORAU under DOE contract number DE-SC0014664. All opinions expressed in this paper are the author's and do not necessarily reflect the policies and views of DOD, DOE, or ORAU/ORISE.

## REFERENCES

- <sup>1</sup> Lubert, C. P., Gee, K. L., and Tsutsumi, S., “Supersonic jet noise from launch vehicles: 50 years since NASA SP-8072,” *J. Acoust. Soc. Am.* **151**(2), 752-791 (2022). doi: [10.1121/10.0009160](https://doi.org/10.1121/10.0009160)
- <sup>2</sup> Jones, N., “Does the roar of rocket launches harm wildlife? These scientists seek answers,” *Nature* **618**, 16-17 (2023). doi: [10.1038/d41586-023-01713-7](https://doi.org/10.1038/d41586-023-01713-7)

- <sup>3</sup> Kantola, R. A., "Acoustic properties of heated twin jets," *J. Sound Vib.* **79**(1), 79-106 (1981). doi: [10.1016/0022-460X\(81\)90330-8](https://doi.org/10.1016/0022-460X(81)90330-8)
- <sup>4</sup> Pineau, P., and Bogey, C., "Acoustic shielding and interaction effects for strongly heated supersonic twin jets," *AIP Advances* **11**, 075114 (2021). doi: [10.1063/5.0059789](https://doi.org/10.1063/5.0059789)
- <sup>5</sup> Greska, B., and Krothapalli, A., "A Comparative Study of Heated Single and Equivalent Twin Jets," *13<sup>th</sup> AIAA/CEAS Aeroacoustics Conference (28<sup>th</sup> AIAA Aeroacoustics Conference)*, 21-23 May 2007, Rome, Italy; AIAA 2007-3634. doi: [10.2514/6.2007-3634](https://doi.org/10.2514/6.2007-3634)
- <sup>6</sup> Bozak, R., "Twin Jet Effects on Noise of Round and Rectangular Jets: Experiment and Model," *20<sup>th</sup> AIAA/CEAS Aeroacoustics Conference*, 16-20 June 2014, Atlanta, GA, USA; AIAA 2014-2890. doi: [10.2514/6.2014-2890](https://doi.org/10.2514/6.2014-2890)
- <sup>7</sup> Eldred, K. M., White, R. W., Mann, M. A., and Cottas, M. G., "Suppression of Jet Noise With Emphasis on the Near Field," ASD-TDR-62-578, Wright-Patterson AFB, Ohio; DTIC Accession Number AD0299026 (1963).
- <sup>8</sup> Kandula, M., "Near-field acoustics of clustered rocket engines," *J. Sound Vib.* **309**(3-5), 852-857 (2008). doi: [10.1016/j.jsv.2007.06.078](https://doi.org/10.1016/j.jsv.2007.06.078)
- <sup>9</sup> Eldred, K. M., "Acoustic loads generated by the propulsion system," NASA SP-8072, Washington, D. C. (1971).
- <sup>10</sup> Potter, R. C., and Crocker, M. J., "Acoustic Prediction Methods for Rocket Engines, Including the Effects of Clustered Engines and Deflected Exhaust Flow," NASA CR-566, Huntsville, AL (1966).
- <sup>11</sup> Katorgin, B. I., Chvanov, V. K., Chelkis, F. J., Popp, M., Tanner, L. G., van Giessen, R. C., and Connaly, S. J., "RD-180 Engine Production and Flight Experience," *40<sup>th</sup> AIAA/ASME/SAE/ASEE Joint Propulsion Conference and Exhibit*, 11-14 July, Fort Lauderdale, FL, USA; AIAA 2004-3998 (2004). doi: [10.2514/6.2004-3998](https://doi.org/10.2514/6.2004-3998)
- <sup>12</sup> Cunningham, C. F., Anderson, M. C., Moats, L. T., Gee, K. L., Hart, G. W., Hall, L. K., and Campbell, S. C., "Acoustical measurement and analysis of an Atlas V launch without solid rocket boosters," *Proc. Mtgs. Acoust.*, in press (2022).
- <sup>13</sup> Gee, K. L., Novakovich, D. J., Mathews, L. T., Anderson, M. C., and Rasband, R. D., "Development of a Weather-Robust Ground-Based System for Sonic Boom Measurements," NASA/CR-2020-5001870, Hampton, VA (2020).
- <sup>14</sup> James, M. M., Salton, A., Calton, M., Downing, M., Gee, K. L., and McNerny, S. A., "Commercial Space Operations Noise and Sonic Boom Measurements," *National Academies of Sciences, Engineering, and Medicine*, Washington, D. C. (2020). doi: [10.17226/25834](https://doi.org/10.17226/25834)
- <sup>15</sup> Anderson, M. C., Gee, K. L., Novakovich, D. J., Mathews, L. T., and Jones, J. T., "Comparing two weather-robust microphone configurations for outdoor measurements," *Proc. Mtgs. Acoust.* **42**, 040005 (2020). doi: [10.1121/2.0001561](https://doi.org/10.1121/2.0001561)
- <sup>16</sup> Gee, K. L., Hart, G. W., Cunningham, C. F., Anderson, M. C., Bassett, M. S., Mathews, L. T., Durrant, J. T., Moats, L. T., Coyle, W. L., Kellison, M. S., and Kuffskie, M. J., "Space Launch System acoustics: Far-field noise measurements of the Artemis-I launch," *JASA Express Lett.* **3**, 023601 (2023). doi: [10.1121/1.2369320](https://doi.org/10.1121/1.2369320)
- <sup>17</sup> Hart, G. W., and Gee, K. L., "Correcting for ground reflections when measuring overall sound power level and acoustic radiation efficiency of rocket launches," *Proc. Mtgs. Acoust.* **50**, 040004 (2022). doi: [10.1121/2.0001733](https://doi.org/10.1121/2.0001733)
- <sup>18</sup> McNerny, S. A., "Launch Vehicle Acoustics Part 1: Overall Levels and Spectral Characteristics," *Journal of Aircraft* **33**(3), 511-517 (1996). doi: [10.2514/3.46974](https://doi.org/10.2514/3.46974)
- <sup>19</sup> Franken, P. A., "Jet Noise," in *Noise Reduction*, edited by L. L. Beranek (McGraw-Hill, New York), Chap. 24, pp. 644-666 (1960). See also Franken, P. A., "Review of Information on Jet Noise," *Noise Control* **4**, 8-16 (1958). doi: [doi.org/10.1121/1.2369320](https://doi.org/10.1121/1.2369320)
- <sup>20</sup> Gurbatov, S. N., and Rudenko, O. V., "Statistical phenomena," in *Nonlinear Acoustics*, edited by M. F. Hamilton and D. T. Blackstock (Academic, San Diego), Chap. 13, pp. 377-398 (1998).
- <sup>21</sup> Anderson, M. C., Gee, K. L., Cunningham, C. F., and Hart, G. W., "Analysis of nonlinear acoustic propagation from an Atlas V launch vehicle," *24<sup>th</sup> International Congress on Acoustics*, 24-28 October, Gyeongju, Korea (2022).
- <sup>22</sup> Coltrin, I. S., Maynes, R. D., Blotter, J. D., and Gee, K. L., "Influence of nozzle spacing and diameter on acoustic radiation from supersonic jets in closely spaced arrays," *Applied Acoustics* **81**, 19-25 (2014). doi: [10.1016/j.apacoust.2014.01.008](https://doi.org/10.1016/j.apacoust.2014.01.008)